

Comparison of aerial parts of *Astragalus membranaceus* and *Astragali Radix* based on chemical constituents and pharmacological effects

Er-Bing Wang, Teng Liu, Xiao-Lin Lu, Jin-Fang Xu, Qian Zheng, Zheng-Bao Zhao & Ting-Li Qu

To cite this article: Er-Bing Wang, Teng Liu, Xiao-Lin Lu, Jin-Fang Xu, Qian Zheng, Zheng-Bao Zhao & Ting-Li Qu (2019) Comparison of aerial parts of *Astragalus membranaceus* and *Astragali Radix* based on chemical constituents and pharmacological effects, *Food and Agricultural Immunology*, 30:1, 1046-1066, DOI: [10.1080/09540105.2019.1663154](https://doi.org/10.1080/09540105.2019.1663154)

To link to this article: <https://doi.org/10.1080/09540105.2019.1663154>



© 2019 The Author(s). Published by Informa UK Limited, trading as Taylor & Francis Group



Published online: 08 Sep 2019.



[Submit your article to this journal](#)



Article views: 729



[View related articles](#)



[View Crossmark data](#)



Citing articles: 3 [View citing articles](#)

Comparison of aerial parts of *Astragalus membranaceus* and *Astragali Radix* based on chemical constituents and pharmacological effects

Er-Bing Wang^a, Teng Liu^b, Xiao-Lin Lu^b, Jin-Fang Xu^b, Qian Zheng^b, Zheng-Bao Zhao^b and Ting-Li Qu^b

^aInstitute of Chemical and Biological Technology, Taiyuan University of Science and Technology, Taiyuan, People's Republic of China; ^bSchool of Pharmaceutical Science of Shanxi Medical University, Taiyuan, People's Republic of China

ABSTRACT

This study aims to provide a scientific basis for the comprehensive utilization of the aerial parts of *Astragalus membranaceus* (APAM). UPLC-Qtrap HRMS was used to identify secondary metabolites in APAM and *Astragali Radix* (AR), the pharmacological effects of them in N-acetyl phenylhydrazine (APH) and cyclophosphamide (Cy)-induced mice were studied by using ¹H NMR-based metabolomics. The results showed that the secondary metabolites of APAM and AR were different, but that there was no difference in the contents of eight constituent flavonoids and four constituent saponins, which were 0.8800 and 4.4351 mg/g in APAM and 0.8944 and 4.6422 mg/g in AR, respectively. APAM and AR induced beneficial effects on the recovery of body weight, blood parameters, viscera indices, Na⁺-K⁺-ATPase, and Ca²⁺-Mg²⁺-ATPase, the blood-enriching mechanisms of them were probably related to valine, leucine, and isoleucine biosynthesis, D-glutamine and D-glutamate metabolism, alanine, aspartate, and glutamate metabolism, and taurine and hypotaurine metabolism.

ARTICLE HISTORY

Received 2 February 2019
Accepted 28 August 2019

KEYWORDS


Aerial parts of *Astragalus membranaceus*; *Astragali radix*; LC/Q Exactive Orbitrap mass spectrometry; metabolomics; Drug efficacy index

1. Introduction

Astragali Radix (AR), which has the Chinese name Huangqi, is derived from the roots of *Astragalus membranaceus* (Fisch.) Bge. or *Astragalus membranaceus* var. *mongholicus* (Bge.) Hsiao., as stated in the Chinese Pharmacopoeia. It has been used for approximately 2000 years in China for the treatment of fatigue, Qi deficiency, anemia, and lack of appetite (Huang et al., 2018; Li, He, Sun, Qin, & Du, 2014; Zhao, Ma, Zhu, Yu, & Weng, 2011).

Aerial parts of *Astragalus membranaceus* (APAM), consisting of stems and leaves, refers to the parts of the plants that are grown above the ground. In our previous study

CONTACT Zheng-Bao Zhao  zhengbao_Z@163.com  School of Pharmaceutical Science of Shanxi Medical University, No.56, Xinjian south Road, Taiyuan 030001, Shanxi, People's Republic of China; Ting-Li Qu  qutingli@126.com  School of Pharmaceutical Science of Shanxi Medical University, No.56, Xinjian south Road, Taiyuan 030001, Shanxi, People's Republic of China

 Supplemental data for this article can be accessed <https://doi.org/10.1080/09540105.2019.1663154>

© 2019 The Author(s). Published by Informa UK Limited, trading as Taylor & Francis Group

This is an Open Access article distributed under the terms of the Creative Commons Attribution-NonCommercial-NoDerivatives License (<http://creativecommons.org/licenses/by-nc-nd/4.0/>), which permits non-commercial re-use, distribution, and reproduction in any medium, provided the original work is properly cited, and is not altered, transformed, or built upon in any way.

(Wang, Zhang, Wu, & Wang, 2017), nuclear magnetic resonance (NMR) was used to compare the chemical composition of APAM and AR. Through the use of ^1H NMR-based metabolomic techniques, the pharmacological effects of APAR and AR were studied in cyclophosphamide (Cy)-treated mice. The results showed that APAM and AR had different metabolite profiles, and some obvious differences in the relative contents of metabolites were observed, but there was no significant difference between their regulation of biomarkers in Cy-treated mice. It is generally known that AR has various pharmaceutical activities; therefore, it is necessary to investigate the difference in biological effects between APAM and AR by using diverse animal models. In addition, the compounds identified by ^1H NMR were mostly primary metabolites; thus, the identification of secondary metabolites in APAM and AR, such as saponins and flavonoids, is also highly desirable.

In recent years, liquid chromatography coupled with mass spectrometry (LC-MS) has emerged as a powerful tool for the analysis of traditional Chinese medicines (TCMs) because of its excellent peak separation, selectivity, and sensitivity (Cheng et al., 2019; He et al., 2018; Wang, Zhang, et al., 2017). LC-MS was used to distinguish between waxy corn and non-waxy corn (Li et al., 2019); therefore, it is undoubtedly a better choice for the identification of the secondary metabolites in APAM and AR. Several LC-MS analytical methods, including LC-ESI/MS, LC-ESI-ion trap/MS, and LC-APCI-TSQ/MS, were used to identify secondary metabolites in AR (Du, Zhao, Zhang, Yao, & Zhang, 2014; Xiao et al., 2011; Zhang, Xiao, Xue, Sun, & Liang, 2007). Ultra-high performance liquid chromatography coupled with Q Exactive Orbitrap-high resolution mass spectrometry (UPLC-Qtrap HRMS) allows the simultaneous acquisition of two different scan types, and provides a higher mass accuracy and mass resolution than any other MS techniques (Shao et al., 2015). Therefore, many studies have described the qualitative analyses of TCMs using UPLC-Qtrap HRMS methods (Adhikari, Boelt, & Fomsgaard, 2016; Zhang et al., 2014).

In the present study, a new UPLC-Qtrap HRMS method was developed to identify the secondary metabolites in APAM and AR, and a ^1H NMR-based metabolomics was used to examine the pharmacological effects of APAR and AR in N-acetyl phenylhydrazine (APH) and Cy-treated mice. In combination with our previous study (Wang, Jin, et al., 2017), the results of this study are expected to contribute significantly to the establishment of a scientific basis for the comprehensive utilization of APAM.

2. Materials and methods

2.1. Chemicals and reagents

Authentic standards of calycosin-7-O- β -D-glycoside (20120428, compound 1), formononetin (20120528, compound 2), (6R, 11R)-3-hydroxy-9,10-dimethoxypterocarpan-3-O- β -D-glucoside (20120515, compound 3), (3R)-7,2'-dihydroxy-3',4'-dimethoxyisoflavan-7-O- β -D-glucoside (20100202, compound 4), (6R,11R)-3-hydroxy-9,10-dimethoxypterocarpan (20120505, compound 7), (3R)-7,2'-dihydroxy-3',4'-dimethoxyisoflavan (20120506, compound 8), astragaloside IV (20120315, compound 9), astragaloside III (20120516, compound 10), astragaloside II (20110503, compound 11), and astragaloside I (20111125, compound 12) were purchased from Shanghai Eternal Biotechnology Co.,

Ltd (Shanghai, China). Calycosin (13082713, compound 5) and ononin (13021808, compound 6) were obtained from Chengdu Manst Company (Sichuan, China).

HPLC-grade acetonitrile was purchased from Merck (Darmstadt, Germany). Methanol was obtained from Beijing Chemical Works (Beijing, China). Ultra-pure water (18 M Ω at 25°C) used in the mobile phase was obtained from a Millipore Alpha-Q water purification system (Millipore, Bedford, MA, USA).

APH was purchased from SangonBiotech Co., Ltd. (Shanghai, China), and Cy was purchased from Jiangsu Hengrui Medicine Co., Ltd (Jiangsu, China). Sodium 3-trimethylsilyl [2,2,3,3-d₄] propionate (TSP) was supplied by Cambridge Isotope Laboratories Inc. (Andover, MA, USA). K₂HPO₄·3H₂O and NaH₂PO₄·2H₂O were purchased from Beijing Chemical Works (Beijing, China). D₂O was supplied by Norell (Landisville, NJ, USA). Assay kits for Na⁺-K⁺-ATPase and Ca²⁺-Mg²⁺-ATPase were purchased from Nanjing Jiancheng Bioengineering Institute (Nanjing, China).

2.2. Plant material

Six batches of APAM and AR (5 years) were collected from Hunyuan County in Shanxi Province in September 2015 from the same planting area, and were authenticated by Prof. Yun-E Bai. The voucher specimens were deposited in the herbarium of the School of Pharmaceutical Science, Shanxi Medical University, until use.

2.3. Chemical constituent analysis

2.3.1. Preparation of standard solutions

Stock solutions. Stock solutions of reference compounds 1–12 were prepared by dissolving the reference standards in methanol at concentrations of 1.870, 1.360, 1.362, 0.601, 0.522, 1.254, 1.226, 1.046, 0.979, 0.500, 0.582, and 1.972 mg/mL, respectively, and then stored at 4°C.

Reference compound mixture solution for UPLC-Qtrap HRMS and HPLC analyses. Aliquots of the 12 stock solutions were mixed and then diluted with methanol to produce the reference compound mixture solution. The concentration of each of the reference compounds 1–12 was 56.5, 81.3, 75.5, 86.8, 19.9, 18.4, 24.5, 83.7, 53.9, 43.7, 63.4, and 108.9 μ g/mL, respectively. The mixture solution was centrifuged at 13,000 rpm for 10 min before UPLC-Qtrap HRMS and HPLC analyses.

2.3.2. Sample preparation

Crude APAM and AR were pulverized into a powder. Each powdered sample (8 g) was extracted under reflux with methanol (100 mL) at 80°C for 1 h. The extraction solution was then concentrated to 10 mL with under vacuum and centrifuged at 13,000 rpm for 10 min before UPLC-Qtrap HRMS and HPLC analyses (Xiong, 2017).

2.3.3. Conditions for qualitative analysis

A UPLC-Qtrap HRMS system (Agilent, MA, USA) with an ESI ion source was used for qualitative analysis. The mobile phase comprised acetonitrile (A) and ultrapure water (B), and the gradient elution conditions were: 0–3 min, 80% B; 3–6 min, 80%–73% B; 6–10 min, 73% B; 10–12 min, 73%–57% B; 12–16 min, 57%–40% B; 16–20 min, 40%–

0% B; 20–24 min, 0% B; 24–26 min, 0%–80% B. Samples were separated by using a ACQUITY UPLC®HSS T3 (1.8 μm , 100 mm \times 2.1 mm, Waters, USA) at 30°C. The flow rate was 0.3 mL/min, and the injection volume was 0.5 μL (Zhang, Li, Qi, Qin, & Li, 2018).

To achieve more structural information, the samples were analyzed in both negative and positive ion modes with the tuning methods set as follows: spray voltage, 3500 V (\pm); sheath gas flow rate, 35 arb; aux gas flow rate, 10 arb; capillary temperature, 330°C. The mass scan range was from m/z 100–1500 (Hu, Xu, Qin, & Liu, 2017).

2.3.4. Conditions for quantitative analysis

HPLC conditions employed were those as previously reported in the literature (Xiong, 2017). HPLC-UV-ELSD analysis was performed by using a Waters e2695 liquid chromatograph to determine the content of eight flavonoids and four saponins. The HPLC instrument consisted of a quaternary pump, an autosampler, and a DAD set at 230 nm coupled with an ELSD (e6000, USA). The separation was achieved on a Venusil MP C₁₈ column (250 mm \times 4.6 mm, 5 μm) operated at 25°C. The injection volume was 20 μL . The following ELSD parameters were set: air pump pressure, 0.5 MPa; nitrogen gas flow, 2.5 L/min; drift tube temperature, 105°C; gain level, 1.0. The mobile phase comprised (A) water and (B) acetonitrile at a flow rate of 1.0 mL/min. The elution conditions were optimized to the following: 20% B, 0–8 min; 20%–30% B, 8–15 min; 30%–43% B, 15–30 min; 43%–60% B, 30–40 min; 60%–100% B, 40–50 min; 100% B, 50–60 min; and 100%–20% B, 60–66 min.

2.4. Pharmacological effects

2.4.1. APAM and AR crude aqueous extract

The crudes of APAM and AR were pulverized into a powder. In accordance with the conventional protocol, each powdered sample (100 g) was extracted twice under reflux (2 h each) with 1000 mL water. The combined aqueous extracts were filtered, concentrated under reduced pressure, and subsequently freeze-dried.

2.4.2. Animal model, drug administration, and sample collection

Thirty-two Kunming mice (18–20 g, 4-week-old) were purchased from the Experimental Animal Centre of Academy of Military Medical Sciences, (License number (Military): SCXK2012-0004). All mice were received humane care throughout the experiment, and were maintained in constant conditions (20°C–24°C; relative humidity, 65% \pm 10%; 12 h light–dark) and given free access to food and water for an acclimation period of 1 week.

The animal experiment was conducted as previously described in the literature, with minor modifications (Li et al., 2015). After acclimation, the mice were randomly allocated into four groups, each containing eight mice: control-treated mice (control group), mice with blood deficiency (model group), mice with blood deficiency treated with APAM (APAM group), and mice with blood deficiency treated with AR (AR group). Mice in the APAM and AR groups were administered the APAM crude extracts (equivalent to 10 g raw materials/kg/day) and AR crude extracts (equivalent to 10 g raw materials/kg/day), respectively, by oral gavage once per day for 10 consecutive days. Mice in the control group and the model group were administered an equal volume of distilled water.

In the model, APAM, and AR groups, mice were hypodermically injected with 2% APH saline solution on Day 1 and Day 4 at doses of 20 and 40 mg/kg, respectively. Two hours after injection on Day 4, the mice were intraperitoneally injected with Cy saline solution (40 mg/kg), and 24 h subsequently on Days 5, 6, and 7.

On Day 10, blood was collected by retro-orbital bleeding into heparin tubes, and the total blood count parameters, including red blood cells (RBC), white blood cells (WBC), hemoglobin (HGB), and hematocrit (HCT), were determined by using a HEMA-VET950FS automatic animal blood analyzer (Lewicki et al., 2018). The mice were then sacrificed and their blood were collected. Blood samples were centrifuged at 13,000 rpm for 10 min, serum was obtained and used for the determination of Na^+ - K^+ -ATPase and Ca^{2+} - Mg^{2+} -ATPase activities. The thymus and spleen were collected, weighed, snap frozen in liquid nitrogen, and stored at -80°C until further analysis.

2.4.3. Metabolomics study

2.4.3.1. Preparation of spleen samples for NMR measurement. By using an ultrasonic cell crusher, approximately 60 mg of spleen was extracted with 900 μL methanol/water (2:1, v/v). After centrifugation (4°C , 13,000 rpm) for 15 min, the supernatant was dried under a nitrogen gas flow. Subsequently, 600 μL phosphate buffer (0.2 M K_2HPO_4 -0.2 M NaH_2PO_4 , pH 7.4, containing 0.01% TSP and 10% D_2O) was added to the dried supernatant. After centrifugation (4°C , 13,000 rpm) for 15 min, 500 μL of the supernatant was transferred into a 5 mm NMR tube for analysis (Qu, Wang, et al., 2016).

2.4.3.2. NMR measurements for spleen. ^1H NMR spectra were recorded on a Bruker 600-MHz AVANCE III NMR spectrometer (600.13 MHz, Bruker, Germany). Spleen samples were analyzed by using noesygpprld pulse sequence, and 64 scans were collected into 65536 data points over an acquisition time of 2.6542 s, with a spectral width of 12345.7 Hz (Qu, Li, Zhao, Li, & Qin, 2016).

2.4.3.3. NMR data processing. ^1H NMR spectra of the spleen were processed by using the MestReNova software (version 8.0.1, Mestrelab Research, Santiago de Compostella, Spain). The phase and baseline distortions were then corrected manually and referenced internally to the chemical shift of TSP at 0.00 ppm. The spectra were divided and the signal integral computed at 0.01 ppm intervals across the region δ 0.50–9.50 ppm. The region of δ 4.68–5.23 ppm was excluded to eliminate the effect of imperfect water presaturation. Normalization to the tissue weights for spleen extracts was conducted prior to analysis.

2.4.4. Multivariate data analysis

The normalized integral values were mean-centered and then subjected to multivariate pattern recognition analysis by using the SIMCA-P 13.0 software package (Umetrics, Sweden). Unsupervised principal component analysis (PCA) was conducted to obtain a general overview of the variance of metabolites and to identify possible outliers. Partial least squares discriminant analysis (PLS-DA) was applied to determine the separation between groups of samples. Orthogonal projection to latent structure-discriminate analysis (OPLS-DA) was also employed to maximize the separation between different treatments. Finally, 200 permutation tests, seven-fold cross-validation, and CV-ANOVA were used to assess the validity of the model.

Relative amounts of metabolites were evaluated based on the integrated regions (buckets) from the least overlapping NMR signals of metabolites. The values of body weight, viscera indices (thymus index and spleen index), blood parameters (WBC, RBC, HGB, and HCT), $\text{Na}^+ - \text{K}^+ - \text{ATPase}$, $\text{Ca}^{2+} - \text{Mg}^{2+} - \text{ATPase}$, and the peak areas (buckets) of the differential metabolites were expressed as the mean \pm standard deviation (SD), and compared by *t*-test using SPSS16.0 software. *P* values of < 0.05 were considered to be statistically significant.

3. Results

3.1. Analysis of chemical constituents of APAM and AR

3.1.1. Qualitative analysis

The total ion chromatograms (TICs) of APAM and AR are illustrated in Figure 1 and Figure 2. The signals were assigned based on comparison of the retention time, fragmentation pathways, and MS/MS spectra with those of reference compounds and previous studies (Liu et al., 2015; Shi et al., 2015; Zhang, Xu, Huang, Zhu, & Qiu, 2015). Twelve compounds were unambiguously assigned by using reference compounds and 32 compounds were tentatively identified (Figure 1, Figure 2, and Table S1).

The compounds identified in APAM and AR were saponins, flavonoids, and carbohydrates. Saponins, including astragaloside IV (peak 33), astragaloside III (peak 34), astragaloside II (peak 39), isoastragaloside II (peak 40), astragaloside I (peak 41), isoastragaloside I (peak 42), astragaloside VIII (peak 43), and acetylastragaloside I (peak 44), were identified. The identified flavonoids included calycosin-7-*O*-D-glucoside (peak 2), odoratin-7-*O*-glycoside (peak 3), trihydroxy-dimethoxyisoflavan-hex (peak 4), 3-hydro-9-MP-hex (peak 5), dihydroxy-trimethoxy DHIF-hex (peak 7), pratensein-7-*O*-

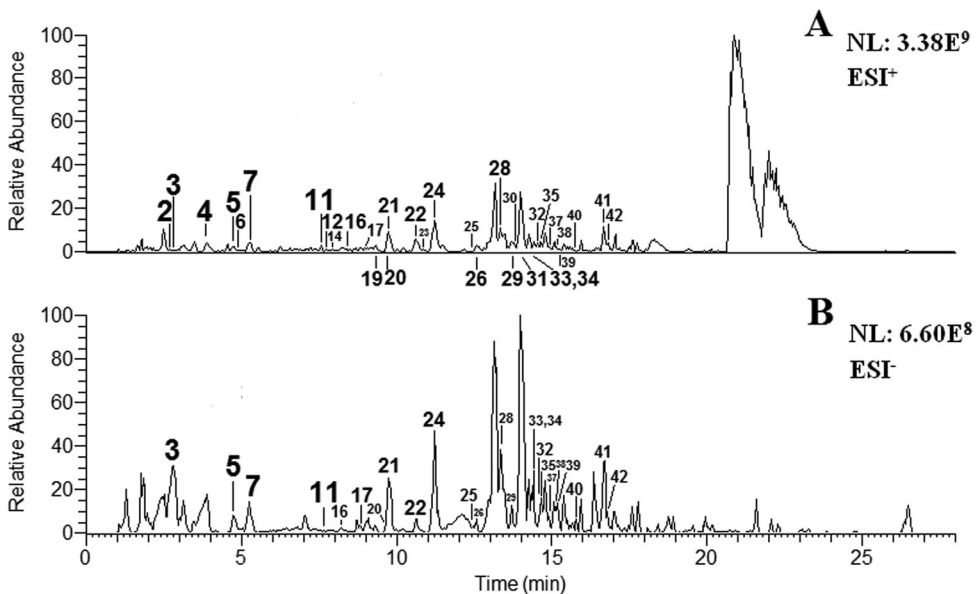


Figure 1. The TICs of base peak of APAM (A: Positive scan; B: Negative scan).

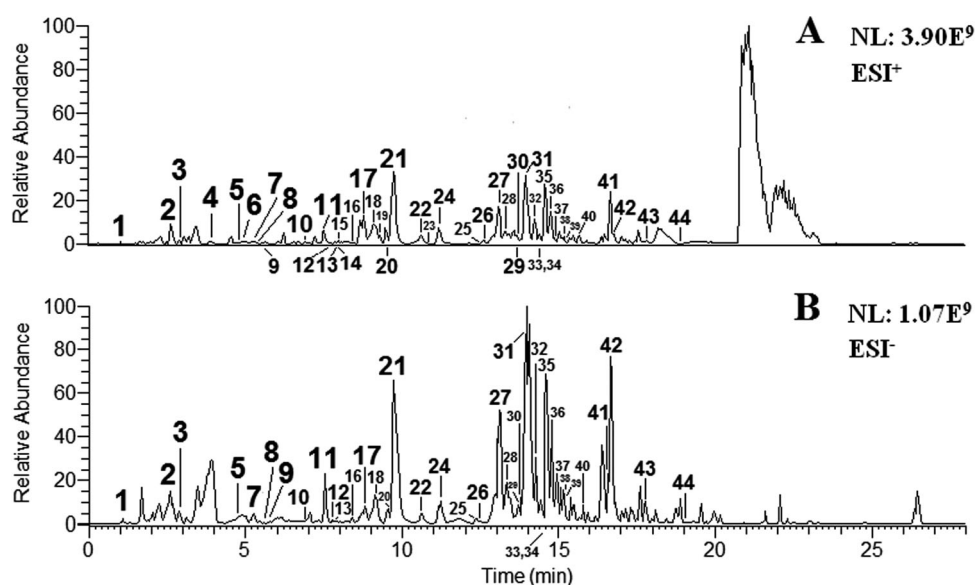


Figure 2. The TICs of base peak of AR (A: Positive scan; B: Negative scan).

glucoside (peak 8), 10-hydroxy-9-methoxypterocarpan-3-*O*- β -D-glycoside (peak 9), odoratin-7-*O*-glycoside-6"-*O*-malonate (peak 10), ononin (peak 11), calycosin-7-*O*- β -D-glycoside-6"-*O*-acetate (peak 12), 6,4'-dimethoxyisoflavone-7-*O*-glucoside (peak 13), 3-hydroxy-9,10-dimp-pen-hex (peak 15), dihydroxyflavone (peak 16), 3-hydroxy-9,10-dimethoxypterocarpan-3-*O*- β -D-glycoside (peak 17), MP (peak 18), isomnronulatol-7-*O*-glucoside (peak 19), 7, 2'-dihydroxy-3',4'-dimethoxy-isoflavan-7-*O*- β -D-glycoside (peak 20), calycosin (peak 21), dihydroxy-dimethoxyisoflavone (peak 22), rhamnocitrin-hex-acetate (peak 23), pratensein (peak 24), 3-hydro-9-MP (peak 25), ononin-6"-*O*-acetate (peak 27), 7-hydroxy-6,4'-dimethoxyisoflavone (peak 28), pratensein-7-*O*-Glc-6"-*O*-acetate (peak 29), 3-hydro-9,10-dimp (peak 30), 4',5',6,7,8-fimethoxy-3',5-dihydroxyflavone (peak 32), formononetin (peak 35), 7-hydroxy-6,4'-dimethoxyisoflavone (peak 36), 3-hydroxy-9, 10-dimethoxypterocarpan (peak 37), 7,2'-dihydroxy-3',4'-dimethoxyisoflavan (peak 38). Sucrose (peak 20) was identified. Of these peaks, 1, 8, 9, 10, 13, 15, 18, 27, 28, 43, and 44 were only detected in AR.

3.1.1.1. Identification of saponins. By comparing the individual chromatographic peak behaviour with these of reference standards, peaks 41, 39, 34, and 33 were unequivocally confirmed as astragaloside I, astragaloside II, astragaloside III, and astragaloside IV, respectively. Taking astragaloside IV as an example, and the proposed fragmentation pathway of astragaloside IV was illustrated (Figure S1). For example, peak 33 was unequivocally identified as astragaloside IV based on its retention time of 14.46 min, which exhibited a molecular ion at m/z 784.46035 ($C_{41}H_{68}O_{14}$), $[M+H]^+$ ion at m/z 785.46704 ($[C_{41}H_{69}O_{14}]^+$, calcd. 785.46818), $[M-H]^+$ ion at m/z 783.45520 ($[C_{41}H_{67}O_{14}]^+$, calcd. 783.45253), and $[M+Cl]^-$ ion at m/z 819.43091 ($[C_{41}H_{68}O_{14}Cl]^-$, calcd. 819.42921). The proposed fragmentation pathway of astragaloside IV is shown in Figure S1. In the positive ion one-level mass spectrogram (Figure S2A), $[M+Na]^+$ ion at m/z 807.44983

confirmed that m/z 785.46704 was the $[M + H]^+$ ion peak. In the positive ion second-level mass spectrogram (Figure S2B), peak 33 displayed an ion at m/z 627.38751 ($[C_{35}H_{56}O_8 - Na]^+$, calcd. 627.38674) from the losses of H_2O and $C_6H_{10}O_5$ of the $[M + Na]^+$ ion at m/z 807.45062, and m/z 495.34482 ($[C_{30}H_{48}O_4Na]^+$, calcd. 495.34448) was the fragment ion due to the loss of $-C_5H_8O_4$ from m/z 627.38751. All eight saponins corresponding to peaks 33, 34, 39, 40, 41, 42, 43, and 44 were identified in this way.

3.1.1.2. Identification of flavonoids. Peak 2 was unequivocally identified as calycosin-7- O - β -D-glycoside, with a retention time of 2.66 min, which showed a precursor ion at m/z 446.12074 ($C_{22}H_{22}O_{10}$), $[M + H]^+$ ion at m/z 447.12833 ($[C_{22}H_{23}O_{10}]^+$, calcd. 447.12857), $[M - H]^+$ ion at m/z 445.11411 ($[C_{22}H_{21}O_{10}]^+$, calcd. 445.11292), and $[M + Cl]^-$ ion at m/z 481.09018 ($[C_{22}H_{22}O_{10}Cl]^-$, calcd. 481.08960). In the positive ion one-level mass spectrogram (Figure S4A), $[M + Na]^+$ ion at m/z 469.11035, and $[2M + Na]^+$ ion at m/z 915.23096 confirmed that m/z 447.12833 was the $[M + H]^+$ ion peak. In the positive ion second-level mass spectrogram (Figure S4B), Peak 2 displayed an ion at m/z 285.07565 ($[C_{16}H_{13}O_5]^+$, calcd. 285.07575) by the loss of $C_6H_{10}O_5$ from m/z 447.12833, which generated fragment ions at m/z 270.05197 ($[C_{15}H_{10}O_5]^+$, calcd. 270.05227), and m/z 253.04916 ($[C_{15}H_9O_4]^+$, calcd. 253.04953) by the losses of the $-CH_3$, and CH_3OH , respectively. The product ion of m/z 137.02335 ($[C_7H_4O_3]^+$, calcd. 137.02332) was the fragment ion by RDA cracking from m/z 285.07565, and m/z 225.05437 ($[C_{14}H_9O_3]^+$, calcd. 225.05462) was the fragment ion by the loss of CO from m/z 253.04916. Thirty-one flavonoids, including peaks 2, 3, 4, 5, 7, 8, 9, 10, 11, 12, 13, 15, 16, 17, 18, 19, 20, 21, 22, 23, 24, 25, 27, 28, 29, 30, 32, 35, 36, 37, and 38, were identified.

3.1.2. Quantitative analysis

The content of four flavonoids, including ononin, calycosin, formononetin, and (3R)-7,2'-dihydroxy-3',4'-dimethoxyisoflavan-7- O - β -D-glucoside, and two saponins, including astragaloside IV and astragaloside III, was higher in APAM, which was consistent with the results of our previous study (Wang, Zhang, et al., 2017). However, there was no significant difference between APAM and AR in the total content of the eight flavonoids (compounds 1–8) and the four saponins (compounds 9–12). The results are shown in Table 1.

Table 1. The contents of twelve compounds of APAM and AR.

| Compound | APAM (mg/g) | AR (mg/g) |
|--|---------------------|---------------------|
| Calycosin-7- O - β -D-glycoside | 0.1320 \pm 0.0012 | 0.3793 \pm 0.021 |
| Ononin | 0.2061 \pm 0.016 | 0.1153 \pm 0.034 |
| (6aR,11aR)-3-hydroxy-9,10-dimethoxypterocarpan-3- O - β -D-glucoside | 0.0731 \pm 0.001 | 0.1036 \pm 0.0027 |
| (3R)-7, 2'-dihydroxy-3',4'-dimethoxyisoflavan-7- O - β -D-glucoside | 0.1641 \pm 0.026 | 0.0342 \pm 0.0032 |
| Calycosin | 0.0482 \pm 0.003 | 0.0117 \pm 0.0056 |
| Formononetin | 0.0093 \pm 0.0013 | 0.0036 \pm 0.0011 |
| (6aR,11aR)-3-hydroxy-9, 10-dimethoxypterocarpan | 0.0224 \pm 0.0032 | 0.0236 \pm 0.0038 |
| (3R)-7,2'-dihydroxy-3',4'-dimethoxyisoflavan | 0.2248 \pm 0.015 | 0.2231 \pm 0.043 |
| Astragaloside IV | 0.2369 \pm 0.035 | 0.1941 \pm 0.042 |
| Astragaloside III | 4.1173 \pm 0.056 | 0.1932 \pm 0.086 |
| Astragaloside II | 0.0324 \pm 0.0034 | 0.1759 \pm 0.065 |
| Astragaloside I | 0.0485 \pm 0.0024 | 4.0790 \pm 0.087 |
| Total flavonoids | 0.8800 | 0.8944 |
| Total saponins | 4.4351 | 4.6422 |

Table 2. Effects of APAM and AR treatment on body weight (unit: g).

| | 0 d | 4 d | 8 d | 10 d |
|---------|--------------|---------------|----------------|----------------|
| Control | 20.85 ± 1.25 | 26.54 ± 1.31 | 28.23 ± 1.11 | 30.43 ± 1.21 |
| Model | 20.65 ± 1.32 | 24.21 ± 1.92* | 20.23 ± 1.24** | 20.54 ± 0.84** |
| APAM | 20.42 ± 1.05 | 25.89 ± 1.65 | 23.43 ± 1.09## | 24.96 ± 1.25## |
| AR | 20.53 ± 1.23 | 25.12 ± 0.89 | 23.04 ± 0.97## | 24.24 ± 0.54## |

Data are expressed as mean ± S.D. of eight mice. Compared with Control group, * $p < 0.05$, ** $p < 0.01$; Compared with Model group, # $p < 0.05$, ## $p < 0.01$.

3.2. Pharmacological effect of APAM and AR

3.2.1. Body weight

The body weight of mice in the control, model, APAM, and AR group is listed in Table 2. Significant differences in the body weight of mice were observed between the control and the other three groups on Day 8, suggesting that APH and Cy caused an observable reduction in body weight. In the APAM and AR groups, the body weight of mice was increased on Day 10, however, it was still lower than that of the control group, and there was no significant differences between them.

3.2.2. Blood parameters

As shown in Figure 3, compared with the control group, significant decreases in WBC, RBC, HGB, and HCT were detected on Day 10 in the model group ($p < 0.01$), indicating that the blood deficiency was successfully induced. In the APAM and AR groups, the levels of WBC, RBC, HGB, and HCT were significantly restored to the control levels, with no significant difference between the APAM and AR groups.

3.2.3. Thymus index and spleen index

Organ index was measured by the ratio of organ weight to body weight. The average values of the thymus index and spleen index are listed in Figure 4A. In the model group, severe atrophy of thymus and spleen were observed. After AR or APAM administration, thymus and spleen indices increased. There was no significant difference between the two groups.

3.2.4. $\text{Na}^+\text{-K}^+\text{-ATPase}$ and $\text{Ca}^{2+}\text{-Mg}^{2+}\text{-ATPase}$ content

As shown in Figure 4B, in the model group, the levels of $\text{Na}^+\text{-K}^+\text{-ATPase}$ and $\text{Ca}^{2+}\text{-Mg}^{2+}\text{-ATPase}$ were reduced by APH and Cy treatment ($p < 0.01$). Compared with the model group, APAM and AR treatment both resulted in significant recovery of $\text{Na}^+\text{-K}^+\text{-ATPase}$ and $\text{Ca}^{2+}\text{-Mg}^{2+}\text{-ATPase}$ content ($p < 0.01$), and there was no significant difference between them.

3.2.5. Metabolomic study

3.2.5.1. Metabolite assignment. Typical ^1H NMR spectra of the spleen of mice in the control and the model groups are shown in Figure 5. NMR signals were assigned to specific metabolites based on the literatures (Guan et al., 2018; Qu, Wang, et al., 2016) and confirmed with the help of NMR databases such as HMDB (<http://www.hmdb.ca/>) and BMRB (<http://www.bmrw.wisc.edu/>). Thirty-three metabolites were detected in the spleen, mainly amino acids, organic acids, choline metabolites, tricarboxylic acid cycle (TCA) intermediates, purines, and organic bases. Endogenous metabolites identified in

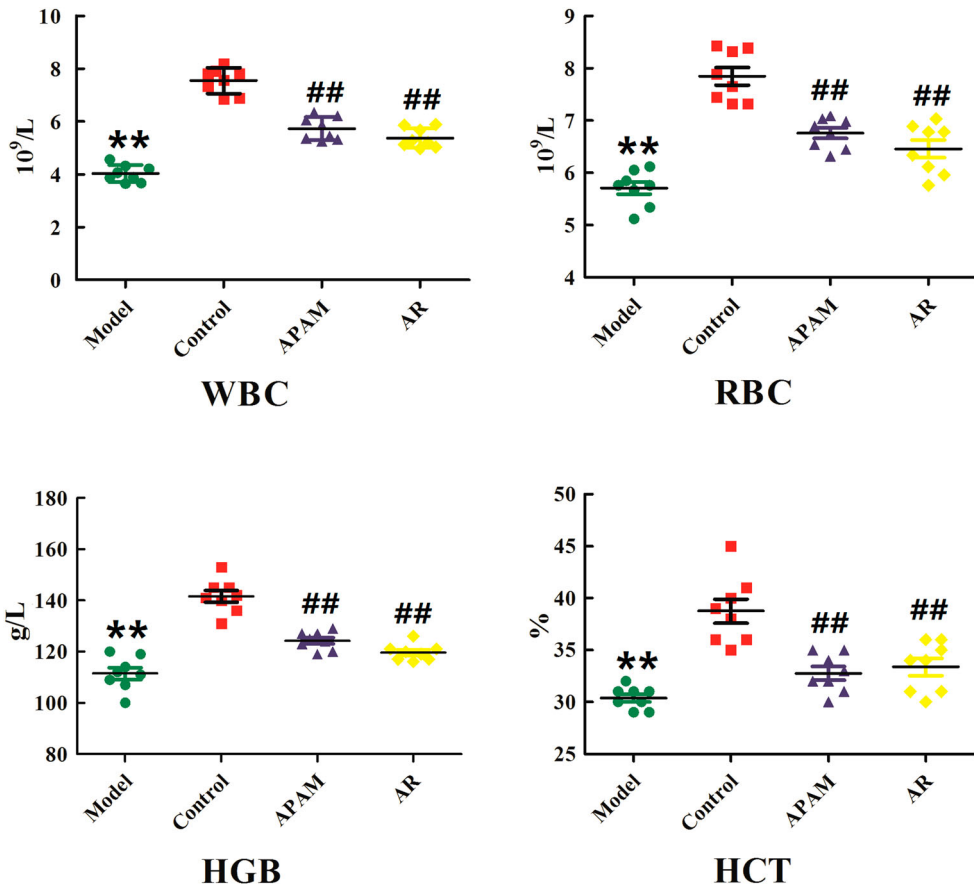


Figure 3. Scatter figures of periphery blood parameters in model, control, APAM and AR groups. Compared with the control group, * $p < 0.05$, ** $p < 0.01$; compared with the model group, # $p < 0.05$, ## $p < 0.01$.

spleen are listed in Table S2. To determine the subtle variations in metabolites, we applied multivariate analysis methods to the NMR data.

3.2.5.2. Metabolomic changes in multiple biological matrices. In the PCA score plot (Figure 6A), clear separation was observed between the control group and the model group, which was generated by PC1 (38.2%) and PC2 (19.5%). PLS-DA and OPLS-DA were applied to maximize the difference between the control group and the model group. In the PLS-DA model, R^2 and Q^2 values were lower than the original ones, suggesting the validity of the discriminant model (Figure 6B). The corresponding OPLS-DA was used to determine the potential biomarkers contributing to the separation (Figure 6C), and the parameters R^2 (0.962), Q^2 (0.895), and p value (2.01×10^{-4}) indicated the interpretability, predictability, and validity of the established model. The OPLS-DA S-plot (Figure 6D), combined with variable importance in the projection (VIP > 1.0), was used to identify the metabolites that contributed to the separation.

Metabolic changes in the spleen contributing to the separation of the model group and the control group mainly involved the elevated content of leucine, isoleucine, valine,

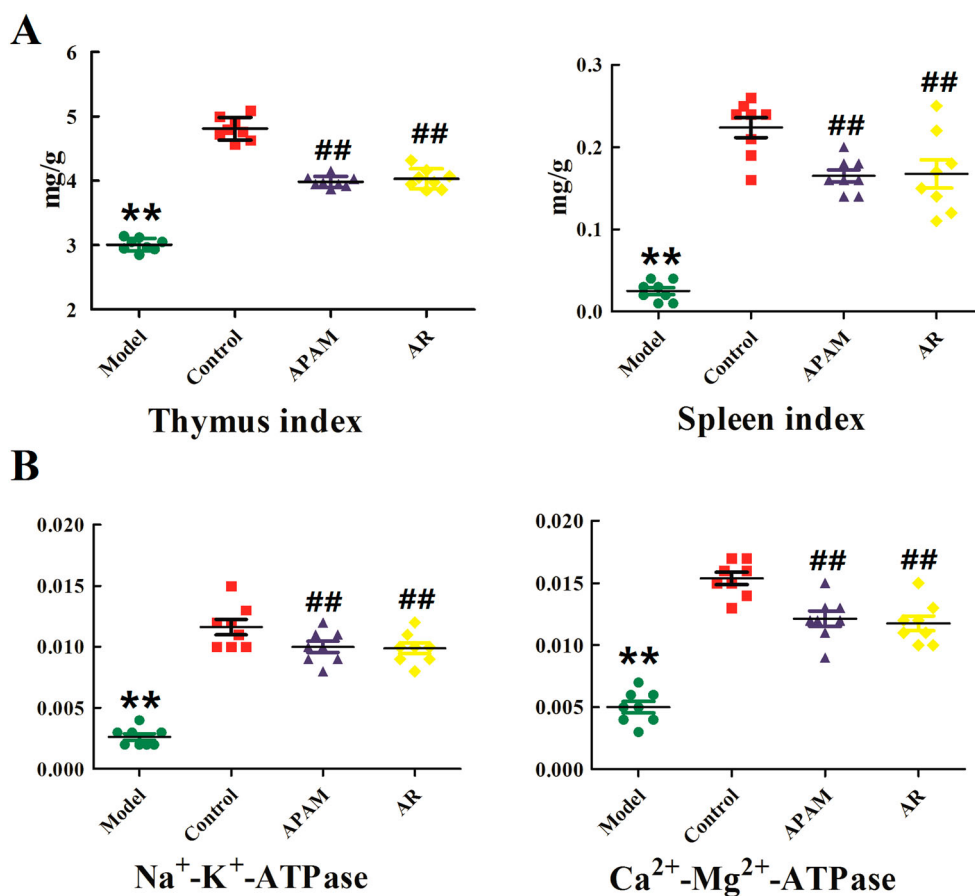


Figure 4. Scatter figure of thymus index, spleen index, Na⁺-K⁺-ATPase, and Ca²⁺-Mg²⁺-ATPase in model, control, APAM and AR groups. Compared with the control group, * $p < 0.05$, ** $p < 0.01$; compared with the model group, # $p < 0.05$, ## $p < 0.01$.

glutamate, methionine, aspartate, creatine, uracil, and uridine in the model group, along with the decreased content of lactate, alanine, arginine, choline, PC, GPC, taurine, and adenosine. The level of each metabolite could be measured by the peak areas (buckets), and was compared by using a *t*-test.

After APAM treatment, the levels of 14 perturbed endogenous metabolites (leucine, isoleucine, valine, lactate, alanine, arginine, glutamate, methionine, aspartic acid, creatine, PC, taurine, uridine, and adenosine) were restored towards the levels in the control group (Table 3). After AR treatment, the levels of 13 perturbed endogenous metabolites (leucine, isoleucine, valine, lactate, alanine, glutamate, methionine, aspartic acid, PC, GPC, taurine, uridine, adenosine) were reversed toward that of the normal controls (Table 3). The efficacy index (EI) was used to compare the effect of enriching the blood by APAM and AR (Xing, Sun, Jia, Qin, & Li, 2017).

$$\text{Efficacy index (EI)} = \sum_{i=1}^n \left| \frac{X_i - M_i}{M_i - C_i} \right| \times 100\%,$$

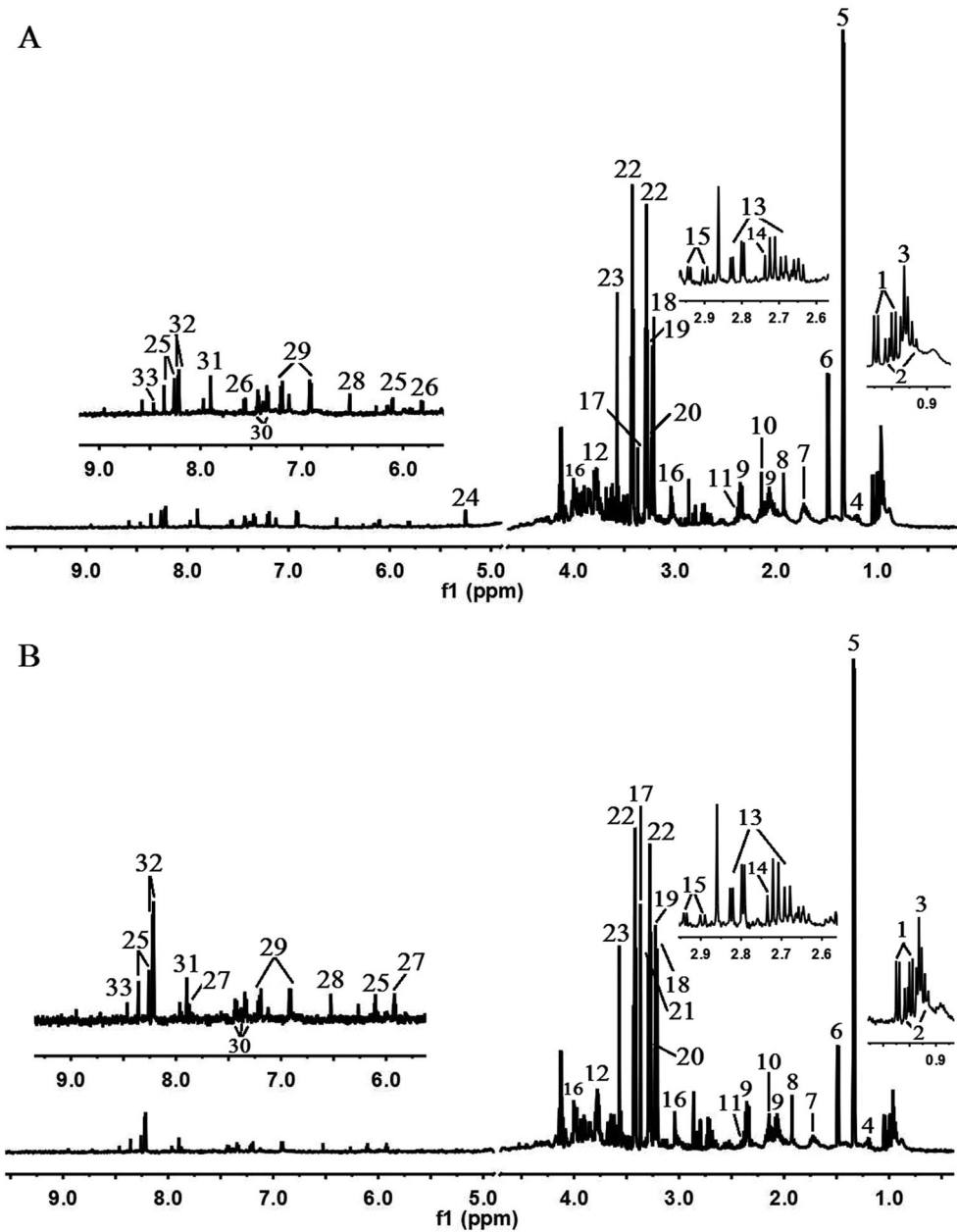


Figure 5. ^1H NMR spectra of spleen from control (A) and model group (B) mice.

where C_i is the average relative content of one of the metabolites in control group; M_i is the average relative content of one of the metabolites in model group; and X_i is the average relative content of one of the metabolites in the APAM or AR groups.

The EI represents the sum of the recovery rate of all recovered metabolites. A higher value of EI indicated a stronger blood enriching effect. As shown in Table 3, the EI of

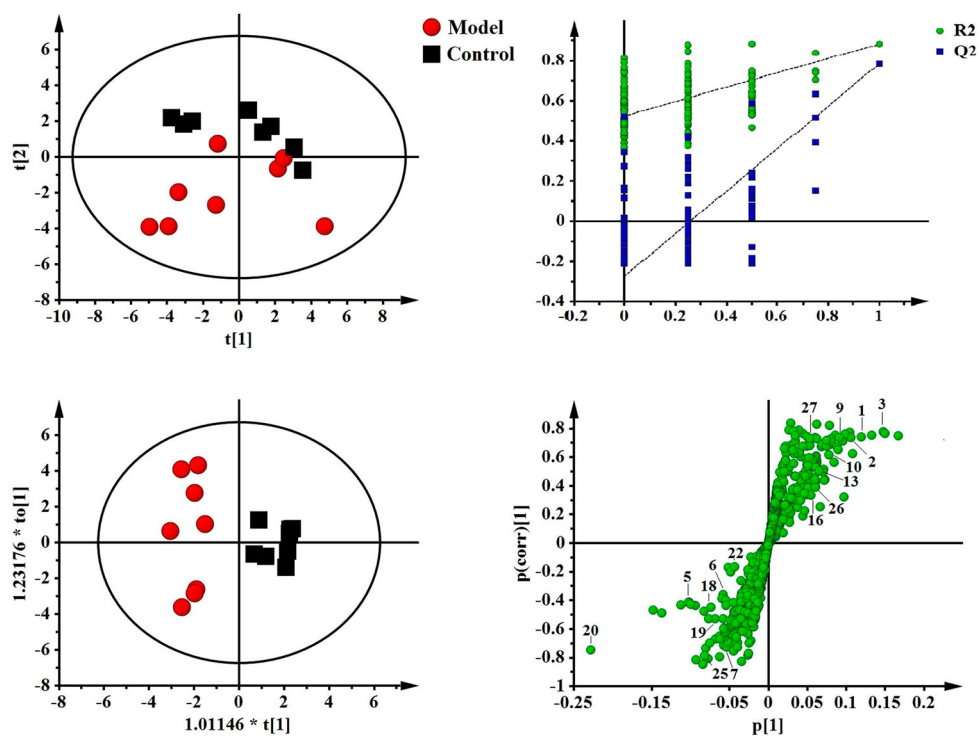


Figure 6. PCA score plot (A), PLS-DA permutation test (B), OPLS-DA score plot (C), and S-plot (D) of mice spleen between the control and model group.

APAM and AR was 1387.79% and 1425.61%, respectively, indicating that APAM and AR had very similar effects on the metabolites recovered.

3.2.5.3. Metabolic pathway analysis. The web-based MetaboAnalyst 3.6 system was used to explore the possible metabolic pathways that were related to blood deficiency. As shown in Figure 7, five metabolic pathways, including valine, leucine, and isoleucine biosynthesis, D-glutamine and D-glutamate metabolism, alanine, aspartate, and glutamate metabolism, taurine and hypotaurine metabolism, and arginine and proline metabolism, with impact values of > 0.1 were filtered out as the most important metabolic pathways.

The recovery of potential metabolites suggested that the effects of APAM and AR on blood deficiency were related to four metabolic pathways: valine, leucine, and isoleucine biosynthesis; D-glutamine and D-glutamate metabolism; alanine, aspartate, and glutamate metabolism; and taurine and hypotaurine metabolism.

4. Discussion

4.1. Analysis of chemical constituents of APAM and AR

It is common knowledge that TCMs contain multiple chemicals, and that their efficacy is the result of the combined action of many chemical components (Liu, 2010). AR was shown to contain more secondary metabolites than APAM, but they had similar blood-

Table 3. The integral levels of metabolites in Control and Model mice in spleen and regulated extent of APAM and AR treated on identified biomarkers.

| $\delta^1\text{H}$ | metabolites | Control | Model | APAM | $X_i - M_i / M_i - C_i$ (APAM) | AR | $X_i - M_i / M_i - C_i$ (AR) |
|--------------------|---------------|-------------------|---------------------|---------------------------------|--------------------------------|---------------------------------|------------------------------|
| 0.96 | Leucine | 0.7234 ± 0.1395 | 0.9665 ± 0.08143** | 0.8167 ± 0.1244 [#] | 0.6162 | 0.7832 ± 0.05134 ^{##} | 0.7540 |
| 1.01 | Isoleucine | 0.4047 ± 0.07575 | 0.5358 ± 0.06132** | 0.3914 ± 0.06295 ^{##} | 1.1014 | 0.4011 ± 0.04608 ^{##} | 1.0275 |
| 1.04 | Valine | 0.2853 ± 0.04570 | 0.3652 ± 0.04600** | 0.2624 ± 0.04702 ^{##} | 1.2866 | 0.2305 ± 0.02618 ^{##} | 1.6859 |
| 1.34 | Lactate | 2.4342 ± 0.5084 | 1.8989 ± 0.08679* | 2.3967 ± 0.1346 ^{##} | 0.9299 | 2.5405 ± 0.2124 ^{##} | 1.1986 |
| 1.48 | Alanine | 0.3296 ± 0.02084 | 0.2326 ± 0.02396** | 0.3516 ± 0.07044 ^{##} | 1.2268 | 0.2952 ± 0.03900 ^{##} | 0.6454 |
| 1.70 | Arginine | 0.1692 ± 0.02901 | 0.1120 ± 0.05652* | 0.1766 ± 0.04323 [#] | 1.1294 | 0.1535 ± 0.03031 | - |
| 2.07 | Glutamate | 0.5723 ± 0.06872 | 0.6230 ± 0.05082* | 0.5898 ± 0.05713 [#] | 0.6548 | 0.5631 ± 0.07379 [#] | 1.1814 |
| 2.15 | Methionine | 0.4846 ± 0.05642 | 0.5726 ± 0.06078* | 0.4412 ± 0.07170 ^{##} | 0.6523 | 0.4145 ± 0.04227 ^{##} | 1.7966 |
| 2.81 | Aspartic acid | 0.1639 ± 0.02662 | 0.2089 ± 0.02245** | 0.1629 ± 0.01681 ^{##} | 1.0222 | 0.1614 ± 0.02026 ^{##} | 1.0556 |
| 3.03 | Creatine | 0.2238 ± 0.03113 | 0.2593 ± 0.02001* | 0.2040 ± 0.03413 ^{##} | 1.5577 | 0.2374 ± 0.05200 | - |
| 3.20 | Choline | 0.2393 ± 0.04962 | 0.1803 ± 0.02645* | 0.2004 ± 0.03254 | - | 0.2072 ± 0.02753 | - |
| 3.22 | PC | 0.4959 ± 0.09506 | 0.3838 ± 0.03346* | 0.4976 ± 0.08780 [#] | 1.0152 | 0.5084 ± 0.09311 ^{##} | 1.1115 |
| 3.23 | GPC | 2.9190 ± 0.3628 | 2.3602 ± 0.3093* | 2.9474 ± 0.7409 | - | 2.6394 ± 0.2626 [#] | 0.4996 |
| 3.27 | Taurine | 1.6534 ± 0.1358 | 1.3736 ± 0.2785* | 1.7347 ± 0.2266 [#] | 1.2906 | 1.7860 ± 0.4135 [#] | 1.4739 |
| 5.82 | Uracil | 0.01307 ± 0.0102 | 0.02768 ± 0.00512* | 0.02556 ± 0.004537 | - | 0.02231 ± 0.01377 | - |
| 5.92 | Uridine | 0.01903 ± 0.00553 | 0.02649 ± 0.00278* | 0.02097 ± 0.00362 ^{##} | 0.7399 | 0.01825 ± 0.00301 ^{##} | 1.1046 |
| 6.11 | Adenosine | 0.06646 ± 0.01262 | 0.04003 ± 0.01301** | 0.05734 ± 0.00828 ^{##} | 0.6549 | 0.05910 ± 0.00345 ^{##} | 0.7215 |

Note: Compared with control group, * $p < 0.05$, ** $p < 0.01$; Compared with model group, [#] $p < 0.05$, ^{##} $p < 0.01$. PC: phosphocholine, GPC: glycerophosphocholine.

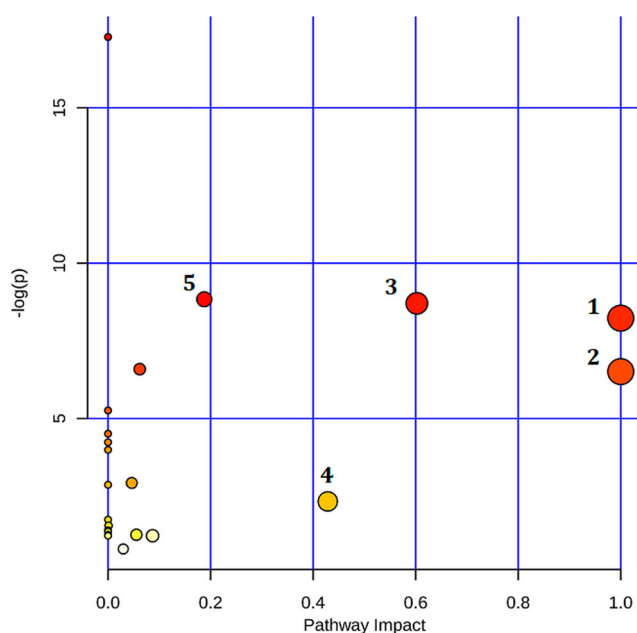


Figure 7. Summary of pathway analysis for differential metabolites (Valine, leucine, and isoleucine biosynthesis (1); D-glutamine and D-glutamate metabolism (2); Alanine, aspartate, and glutamate metabolism (3); Taurine and hypotaurine metabolism (4); Arginine and proline metabolism (5)).

enriching effect. A possible reason for this may be that these compounds can be converted into each other in the body. For example, astragaloside I and astragaloside II may be converted into astragaloside IV, and calycosin-7-O- β -D-glycoside can be hydrolyzed to produce calycosin (Liu et al., 2015). It may also be possible that the blood enriching effect produced by AR was mainly associated with the 12 chemical components that we have determined. It is clear that more in-depth research is required.

4.2. Blood enriching effect of APAM and AR

Cy is a commonly used alkylating agent in chemotherapy for various cancers and autoimmune disorders (Parka et al., 2019). APH, a strong oxidant, exerts slow and progressive oxidative damage on RBC (Li et al., 2015). In the present study, the combination of Cy and APH was used to induce a model of blood deficiency, which was consistent with the internal environment of blood deficiency (Li, Guo, et al., 2014). RBC, WBC, HGB, and HCT are the main diagnostic criteria for blood deficiency syndrome (Ashour, 2014). As $\text{Na}^+\text{-K}^+\text{-ATPase}$ and $\text{Ca}^{2+}\text{-Mg}^{2+}\text{-ATPase}$ are related to blood cells, they are closely associated with anemia (Ji et al., 2018). In our work, pharmacological indicators such as weight, viscera indices, blood parameters, the content of $\text{Na}^+\text{-K}^+\text{-ATPase}$ and $\text{Ca}^{2+}\text{-Mg}^{2+}\text{-ATPase}$, and the recovery of potential metabolites all showed that APAM and AR had comparable blood enriching effects. The current findings agreed with previous studies (Liu et al., 2018; Sun, Xie, Liu, Xu, & Wang, 2003), which showed that AR exerted beneficial effects in the recovery of blood parameters in blood-deficient mice.

4.3. Metabolic pathway changes induced by APAM and AR

The beneficial effects of APAM and AR on blood deficiency may stem from their involvement in some or all the four metabolic pathways, namely valine, leucine, and isoleucine biosynthesis, D-glutamine and D-glutamate metabolism, alanine, aspartate, and glutamate metabolism, and taurine and hypotaurine metabolism.

4.3.1. Valine, leucine, and isoleucine biosynthesis

Valine is an essential amino acid and a raw sugar amino acid (Lv & Guo, 2013). Valine can regulate blood sugar levels and provide an energy supply for the body. In blood deficiency, valine provides extra energy to the muscle for glucose production, which can prevent muscle weakness (Ji et al., 2018). Leucine and isoleucine are important ketogenic amino acids, they can be converted to the metabolite intermediate product 3-hydroxybutyric acid (3-HB) for energy production (Shi, Xiao, Wang, & Tang, 2013).

In this study, significant increases in valine, leucine, and isoleucine were observed in the model group, suggesting that APH and Cy might influence the energy supply in mice, which was in agreement with a report that found increased level of valine in blood deficiency mice (Li et al., 2015). APAM or AR treatment restored the content of valine, leucine, and isoleucine towards that of the normal controls. Previous studies showed that APH and Cy could cause ischemia and anoxia in blood deficiency, which may enhance anaerobic glycolysis (Wang, Sun, Hua, Li, & Wei, 2016). It is suggested that the blood enriching ability of APAM and AR may improve energy metabolism through alteration of the valine, leucine, and isoleucine biosynthesis pathway, which is the most important metabolic pathway related to blood deficiency (Hua, Yao, Ji, & Wei, 2017; Zhang et al., 2019).

4.3.2. D-Glutamine and D-glutamate metabolism

Glutamate is an intermediate product of glutamine metabolism (Wang, Jin, et al., 2017) and may affect the immune response of monocytes/macrophages, the proliferation of lymphocytes, and the synthesis of Hsp70 (Exner et al., 2003). Glutathione (GSH), a tripeptide of glutamate, glycine, and cysteine, is an efficient antioxidant that provides protection against oxidative stress, either by serving as a cofactor for some antioxidant enzymes or by reducing reactive oxygen species (ROS) (Lu, 2013; Roth et al., 2002; Yuan & Kaplowitz, 2009). Disorders of glutamate and glutamine may inhibit the synthesis of GSH, and subsequently lead to high levels of ROS (Guo et al., 2015). However, excessive ROS can disrupt the structure and function of membranes, eventually leading to cell death (Hua et al., 2017).

In this study, the level of glutamate was increased significantly in the model group compared with the control group and was upregulated after treatment of APAM or AR. It is revealed that APAM and AR might relieve the blood deficiency syndrome through alteration of D-glutamine and D-glutamate metabolism.

4.3.3. Alanine, aspartate, and glutamate metabolism

Alanine is an important non-essential amino acid in the body and is a significant element of lymphocyte regeneration and immunologic processes (Newsholme, Bender, Kiely, & Brennan, 2007). Aspartic acid is an α -amino acid and used in the synthesis of threonine

and methionine (Ji et al., 2018). Methionine can enhance the activity of glutathione peroxidase and superoxide dismutase to increase the biosynthesis of GSH (Ji, 2015), which acts as an important antioxidant in human body and has the functions of anti-oxidation, anti-apoptosis and inhibition of inflammatory reaction (Chen et al., 2019; Lu, 2013).

The model group showed higher levels of methionine and aspartic acid and lower level of alanine; these results agreed with a previous report (Ji, 2015). In the APAM and AR groups, the levels of alanine, methionine, and aspartate tended to be restored towards those in the normal control mice, illustrating that APAM and AR might increase the content of alanine to improve immune function and subsequently to enrich blood, and reduce the levels of methionine and aspartate to relieve the blood deficiency syndrome induced by antioxidants.

4.3.4. Taurine and hypotaurine metabolism

Taurine is an important amino acid and is involved in numerous physiological processes, including participating in energy metabolism, maintaining the balance of intracellular osmotic pressure, stabilizing the cell membrane, removing oxygen radicals, maintaining intracellular calcium homeostasis, participating in body temperature regulation, and regulating the sensitivity of insulin (Froger et al., 2014; Huxtable, 1992).

The finding of the reduced taurine level in the model group agreed with previous studies (Wang et al., 2010; Zong et al., 2009), suggesting that more taurine is required to maintain the stability of the cell membrane (Nicholson & Wilson, 2003). Both APAM and AR restored the taurine content toward that of normal control mice and there was no significant difference between them, indicating that APAM and AR had similar effects on taurine and hypotaurine metabolism.

5. Conclusions

In the present study, secondary metabolites in APAM and AR, including saponins and flavonoids, were identified and analyzed by using the UPLC-Qtrap HRMS method, and the biological effects of APAM and AR were compared in the APH and Cy-induced blood deficiency model coupled with ^1H NMR-based metabolomics. The results of this work revealed that the secondary metabolites of APAM and AR were different. However, there was no significant difference in the quantity of the eight flavonoids and the four saponins we analyzed. APAM and AR exerted similar pharmacological effects on blood deficiency induced by APH and Cy, and the mechanism of the blood enriching effect may be related to valine, leucine, and isoleucine biosynthesis, D-glutamine and D-glutamate metabolism, alanine, aspartate, and glutamate metabolism, and taurine and hypotaurine metabolism. In combination with our previous study, this work is expected to provide further evidence for the clinical application of APAM.

Chemical analysis showed that various primary metabolites and secondary metabolites were present in APAM and AR. Although APAM contained fewer chemical components than AR, APAM exerted similar pharmacological effects to AR. This similarity may be related to the metabolic transformation of these compounds in the body. Therefore, it is necessary to compare the metabolism of APAM and AR in the body in future studies in this field.

Acknowledgments

This study was financially supported by School Reform Project of Shanxi Medical University (No. XJ2018064), National Natural Science Foundation of China (No. 31700306), and Shanxi Province Science Foundation for Youths (No. 201701D221256).

Disclosure statement

No potential conflict of interest was reported by the authors.

Funding

This work was supported by National Natural Science Foundation of China: [Grant Number No. 31700306]; School Reform Project of Shanxi Medical University: [Grant Number XJ2018064]; Shanxi Province Science Foundation for Youths: [Grant Number 201701D221256].

References

- Adhikari, K. B., Boelt, B., & Fomsgaard, I. S. (2016). Identification and quantification of Loline-Type Alkaloids in endophyte-infected grasses by LC-MS/MS. *Journal of Agriculture and Food Chemistry*, 64, 6212–6218. doi:10.1021/acs.jafc.6b02616
- Ashour, T. H. (2014). Hematinic and anti-anemic effect of thymoquinone against phenylhydrazine-induced hemolytic anemia in rats. *Research Journal of Medical Sciences*, 8, 67–72.
- Chen, J., Ye, C., Hu, X. M., Huang, C. H., Yang, Z., Li, P. Y., ... Yang, H. M. (2019). Serum metabolomics model and its metabolic characteristics in patients with different syndromes of dyslipidemia based on nuclear magnetic resonance. *Journal of Pharmaceutical and Biomedical Analysis*, 167, 100–113. doi:10.1016/j.jpba.2018.12.042
- Cheng, C. C., Li, R. K., Heng Leung, G. P., Li, S. L., Kong, M., Lao, L. X., ... Meng, W. (2019). Application of UPLC-MS/MS to simultaneously detect four bioactive compounds in the tumour-shrinking decoction (FM1523) for uterine fibroids treatment. *Phytochemical Analysis*, 1–9. doi:10.1002/pca.2827
- Du, H. W., Zhao, X. L., Zhang, A. H., Yao, L., & Zhang, Y. Y. (2014). Rapid separation, identification and analysis of *Astragalus membranaceus* Fisch using liquid chromatography-tandem mass spectrometry. *Journal of Chromatographic Science*, 52, 226–231. doi:10.1093/chromsci/bmt016
- Exner, R., Tamandl, D., Goetzinger, P., Mittlboeck, M., Fuegger, R., Sautner, T., ... Roth, E. (2003). Perioperative Gly-Gln infusion diminishes the surgery-induced period of immunosuppression. *Annals of Surgery*, 237, 110–115. doi:10.1097/01.SLA.0000041040.98684.CB
- Froger, N., Moutsimilli, L., Cadetti, L., Jammoul, F., Gaucher, D., Rosolen, S. G., ... Picaud, S. (2014). Taurine: The comeback of a nutraceutical in the prevention of retinal degenerations. *Progress in Retinal and Eye Research*, 41, 44–63. doi:10.1016/j.preteyeres.2014.03.001
- Guan, Z. B., Wu, J., Wang, C. C., Zhang, F., Wang, Y. N., Wang, M., ... Zhao, C. J. (2018). Investigation of the preventive effect of Sijunzi decoction on mitomycin C-induced immunotoxicity in rats by ¹H NMR and MS-based untargeted metabolomic analysis. *Journal of Ethnopharmacology*, 210, 179–191. doi:10.1016/j.jep.2017.08.021
- Guo, P. P., Wei, D. D., Wang, J. S., Dong, G., Zhang, Q., Yang, M. H., & Kong, L. Y. (2015). Chronic toxicity of crude ricinine in rats assessed by ¹H NMR metabolomics analysis. *RSC Advances*, 5, 27018–27028. doi:10.1039/C4RA14660C
- He, M. Z., Jia, J., Li, J. M., Wu, B., Huang, W. P., Liu, M., ... Feng, Y. L. (2018). Application of characteristic ion filtering with ultra-high performance liquid chromatography quadrupole time of flight tandem mass spectrometry for rapid detection and identification of chemical profiling in *Eucommia ulmoides* Oliv. *Journal of Chromatography A*, 1554, 81–91. doi:10.1016/j.chroma.2018.04.036

- Hu, Y. H., Xu, W. Q., Qin, X. M., & Liu, Y. T. (2017). Rapid identification of chemical constituents in Huangqi Jianzhong Tang by UHPLC coupled with hybrid quadrupole-orbitrap MS. *Acta Pharmaceutica Sinica*, 52, 964–970.
- Hua, Y. L., Yao, W. L., Ji, P., & Wei, Y. M. (2017). Integrated metabonomic-proteomic studies on blood enrichment effects of *Angelica sinensis* on a blood deficiency mice model. *Pharmaceutical Biology*, 55, 853–863. doi:10.1080/13880209.2017.1281969
- Huang, J., Yin, L., Dong, L., Quan, H. F., Chen, R., Hu, S. Y., ... Fu, X. Y. (2018). Quality evaluation for *Radix Astragali* based on fingerprint, indicative components selection and QAMS. *Biomedical Chromatography*, 32, e4343. doi:10.1002/bmc.4343
- Huxtable, R. J. (1992). Physiological actions of taurine. *Physiological Reviews*, 72, 101–163. doi:10.1152/physrev.1992.72.1.101
- Ji, P. (2015). *Metabonomics studies on blood deficiency mice model intervened with Angelica sinensis and its different processed products*. Gansu: Gansu agriculture University.
- Ji, P., Wei, Y. M., Hua, Y. L., Zhang, X. S., Yao, W. L., Ma, Q., ... Yang, C. X. (2018). A novel approach using metabolomics coupled with hematological and biochemical parameters to explain the enriching-blood effect and mechanism of unprocessed *Angelica sinensis* and its 4 kinds of processed products. *Journal of Ethnopharmacology*, 211, 101–116. doi:10.1016/j.jep.2017.09.028
- Lewicki, S., Leśniak, M., Bertrandt, J., Kalicki, B., Kubiak, J. Z., & Lewicka, A. (2018). The long-term effect of a protein-deficient-diet enriched with vitamin B6 on the blood parameters in unexercised and exercised rats. *Food and Agricultural Immunology*, 29, 722–734. doi:10.1080/09540105.2018.1439900
- Li, W. X., Guo, J. M., Tang, Y. P., Shang, E. X., Qian, Y. F., Wang, L. Y., ... Duan, J. A. (2014). Comparative metabolomics analysis on hematopoietic functions of herb pair *Gui-Xiong* by ultra-high-performance liquid chromatography coupled to quadrupole time-of-flight mass spectrometry and pattern recognition approach. *Journal of Chromatography A*, 1346, 49–56. doi:10.1016/j.chroma.2014.04.042
- Li, Q. L., He, Z. Y., Luo, R. T., Nie, T., Zhang, Q. J., Xu, Y., ... Qi, S. W. (2019). Liquid chromatography combined with pattern recognition to detect the metabolic profiling of corn kernels. *Food and Agricultural Immunology*, 30, 713–726. doi:10.1080/09540105.2019.1625874
- Li, Z. Y., He, P., Sun, H. F., Qin, X. M., & Du, G. H. (2014). ¹H NMR based metabolomic study of the antifatigue effect of *Astragali Radix*. *Molecular BioSystem*, 10, 3022–3030. doi:10.1039/c4mb00370e
- Li, P. L., Sun, H. G., Hua, Y. L., Ji, P., Zhang, L., Li, J. X., & Wei, Y. M. (2015). Metabolomics study of hematopoietic function of *Angelica sinensis* on blood deficiency mice model. *Journal of Ethnopharmacology*, 166, 261–269. doi:10.1016/j.jep.2015.03.010
- Liu, G. Z. (2010). *Strategies for global qualitative analysis of flavonoids in traditional Chinese medicines*. Hunan: Hunan Normal University.
- Liu, W. P., Li, C. Y., Huang, J., Liao, J. Z., Liao, S. Y., Ma, W. J., ... Rui, W. (2018). Application of pathways activity profiling to urine metabolomics for screening Qi-tonifying biomarkers and metabolic pathways of honey-processed *Astragalus*. *Journal of Separation Science*, 41, 2661–2671. doi:10.1002/jssc.201701371
- Liu, M. H., Li, P. L., Zeng, X., Wu, H. X., Su, W. W., & He, J. Y. (2015). Identification and pharmacokinetics of multiple potential bioactive constituents after oral administration of *Radix Astragali* on cyclophosphamide-induced immunosuppression in Balb/c mice. *International Journal of Molecular Sciences*, 16, 5047–5071. doi:10.3390/ijms16035047
- Lu, S. C. (2013). Glutathione synthesis. *Biochimica et Biophysica Acta-General Subjects*, 1830, 3143–3153. doi:10.1016/j.bbagen.2012.09.008
- Lv, Z. Q., & Guo, F. F. (2013). Research progress on amino acid sensing and its role in the regulation of glucose and lipid metabolism. *Chinese Bull Life Science*, 2, 004. doi:10.13376/j.cbls/2013.02.002
- Newsholme, P., Bender, K., Kiely, A., & Brennan, L. (2007). Amino acid metabolism, insulin secretion and diabetes. *Biochemical Society Transactions*, 35, 1180–1186. doi:10.1042/BST0351180

- Nicholson, J. K., & Wilson, I. D. (2003). Opinion: Understanding 'global' systems biology: Metabonomics and the continuum of metabolism. *Nature Reviews Drug Discovery*, 2, 668–676.
- Parka, Y. M., Leea, H. Y., Kanga, Y. G., Parkb, S. H., Leeb, B. G., Parkb, Y. J., ... Leef, Y. R. (2019). Immune-enhancing effects of *Portulaca oleracea* L.-based complex extract in cyclophosphamide-induced splenocytes and immunosuppressed rats. *Food and Agricultural Immunology*, 30, 13–24. doi:10.1080/09540105.2018.1540552
- Qu, T. L., Li, Z. Y., Zhao, S. J., Li, A. P., & Qin, X. M. (2016). A metabonomic analysis reveals novel regulatory mechanism of Huangqi injection on leucopenia mice. *Immunopharmacology and Immunotoxicology*, 38, 113–123. doi:10.3109/08923973.2015.1128950
- Qu, T. L., Wang, E. B., Li, A. P., Du, G. H., Li, Z. Y., & Qin, X. M. (2016). NMR based metabolomic approach revealed cyclophosphamide-induced systematic alterations in a rat model. *RSC Advances*, 6, 111020–111030. doi:10.1039/c6ra18600a
- Roth, E., Oehler, R., Manhart, N., Exner, R., Wessner, B., Strasser, E., & Spittler, A. (2002). Regulatory potential of glutamine-relation to glutathione metabolism. *Nutrition*, 18, 217–221.
- Shao, Y. P., Zhu, B., Zheng, R. Y., Zhao, X. J., Yin, P. Y., Lu, X., ... Yao, Z. Z. (2015). Development of urinary pseudotargeted LC-MS-based metabolomics method and its application in hepatocellular carcinoma biomarker discovery. *Journal of Proteome Research*, 14, 906–916. doi:10.1021/pr500973d
- Shi, X. H., Xiao, C. N., Wang, Y. L., & Tang, H. R. (2013). Gallic acid intake induces alterations to systems metabolism in rats. *Journal of Proteome Research*, 12, 991–1006. doi:10.1021/pr301041k
- Shi, J., Zheng, L., Lin, Z. F., Hou, C. Q., Liu, W. Q., Yan, T. M., ... Liu, Z. Q. (2015). Study of pharmacokinetic profiles and characteristics of active components and their metabolites in rat plasma following oral administration of the water extract of *Astragali radix* using UPLC-MS/MS. *Journal of Ethnopharmacology*, 169, 183–194. doi:10.1016/j.jep.2015.04.019
- Sun, Y., Xie, Q. M., Liu, X. M., Xu, F., & Wang, D. J. (2003). Invigorating qi and promoting blood effect of *Astragalus membranaceus* in animal model of blood deficient. *Chinese Journal of Clinical Science*, 15, 2148–2149.
- Wang, E. B., Jin, B. F., Li, X., Liu, R. L., Xie, X. R., Guo, W. F., ... Zhao, Z. B. (2017). Comparative analysis between aerial parts and roots (*Astragali Radix*) of *astragalus membranaceus* by NMR-based metabolomics. *Food and Agricultural Immunology*, 28, 1126–1141. doi:10.1080/09540105.2017.1332007
- Wang, M., Rang, W. Q., Zhang, Q., Huo, C., Ma, Z. C., Wang, Y. G., ... Gao, Y. (2010). NMR-spectroscopy based metabonomic approach to analysis of Siwutang, an ovel prescription, treated blood deficiency in mice. *China Journal of Chinese Materia Medica*, 5, 630–634.
- Wang, T., Sun, H. G., Hua, Y. L., Li, P. L., & Wei, Y. M. (2016). Urine metabonomic study for blood-replenishing mechanism of *Angelica sinensis* in a blood-deficient mouse model. *Chinese Journal of Natural Medicines*, 14, 0210–0219. doi:10.1016/S1875-5364(16)30018-8
- Wang, C. H., Zhang, J. L., Wu, C. S., & Wang, Z. (2017). A multiple-dimension liquid chromatography coupled with mass spectrometry data strategy for the rapid discovery and identification of unknown compounds from a Chinese herbal formula (*Er-xian* decoction). *Journal of Chromatography A*, 1518, 59–69. doi:10.1016/j.chroma.2017.08.072
- Xiao, W. L., Motley, T. J., Unachukwu, U. J., Lau, C. B., Jiang, B., Hong, F., ... Kennelly, E. J. (2011). Chemical and genetic assessment of variability in commercial *Radix Astragali* (*Astragalus* spp.) by ion trap LC-MS and nuclear ribosomal DNA barcoding sequence analyses. *Journal of Agriculture and Food Chemistry*, 59, 1548–1556. doi:10.1021/jf1028174
- Xing, J., Sun, H. M., Jia, J. P., Qin, X. M., & Li, Z. Y. (2017). Integrative hepatoprotective efficacy comparison of raw and vinegar-baked *Radix Bupleuri* using nuclear magnetic resonance-based metabolomics. *Journal of Pharmaceutical and Biomedical Analysis*, 138, 215–222. doi:10.1016/j.jpba.2017.02.015
- Xiong, Y. F. (2017). *Establishment of standard detection procedure for Astragalus saponins and study on the accumulation and distribution of indicator component of Astragalus membranaceus in Hengshan mountain*. Shanxi: Shanxi University.
- Yuan, L. Y., & Kaplowitz, N. (2009). Glutathione in liver diseases and hepatotoxicity. *Molecular Aspects of Medicine*, 30, 29–41. doi:10.1016/j.mam.2008.08.003

- Zhang, Y., Fei, Q. Q., Wang, J., Zhu, F. X., Chen, Y., Tang, D. Q., & Chen, B. (2019). Study on blood enrichment mechanism of steamed notoginseng based on metabolomics method. *China Journal of Chinese Materia Medica*, 44, 2139–2148. doi:10.19540/j.cnki.cjcmm.20190115.001
- Zhang, W. N., Li, A. P., Qi, Y. S., Qin, X. M., & Li, Z. Y. (2018). Metabolomics coupled with system pharmacology reveal the protective effect of total flavonoids of Astragali Radix against dexamethasone-induced rat nephropathy model. *Journal of Pharmaceutical and Biomedical Analysis*, 158, 128–136. doi:10.1016/j.jpba.2018.05.045
- Zhang, J. Y., Wang, Z. J., Zhang, Q., Wang, F., Ma, Q., Lin, Z. Z., ... Qiao, Y. J. (2014). Rapid screening and identification of target constituents using full scan-parent ions list-dynamic exclusion acquisition coupled to diagnostic product ions analysis on a hybrid LTQ-Orbitrap mass spectrometer. *Talanta*, 124, 111–122. doi:10.1016/j.talanta.2013.11.025
- Zhang, X., Xiao, H. B., Xue, X. Y., Sun, Y. G., & Liang, X. M. (2007). Simultaneous characterization of isoflavonoids and astragalosides in two Astragalus species by high performance liquid chromatography coupled with atmospheric pressure chemical ionization tandem mass spectrometry. *Journal of Separation Science*, 30, 2059–2069. doi:10.1002/jssc.200700014
- Zhang, J., Xu, X. J., Huang, J., Zhu, D. Y., & Qiu, X. H. (2015). Rapid Characterization and identification of flavonoids in Radix Astragali by Ultra-high-pressure liquid chromatography coupled with Linear Ion trap-Orbitrap mass spectrometry. *Journal of Chromatographic Science*, 53, 945–952. doi:10.1093/chromsci/bmu155
- Zhao, L. H., Ma, Z. X., Zhu, J., Yu, X. H., & Weng, D. P. (2011). Characterization of polysaccharide from Astragalus radix as the macrophage stimulator. *Cellular Immunology*, 271, 329–334. doi:10.1016/j.cellimm.2011.07.011
- Zong, K. Q., Wang, M., Zhang, Q., Kong, F., Ma, Z. C., Rang, W. Q., ... Gao, Y. (2009). A Metabonomics approach to the analysis of cyclophosphamide induced blood deficiency in BALB/c mice. *Chinese Pharmacological Bulletin*, 25, 61–65.